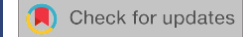
Time-resolved photoelectron spectroscopy of iodide–4-thiouracil cluster: The $\pi\pi^*$ state as a doorway for electron attachment \Box

Megan Asplund [0]; Masafumi Koga [0]; Ying Jung Wu [0]; Daniel M. Neumark []



J. Chem. Phys. 160, 054301 (2024) https://doi.org/10.1063/5.0187557

View	Export
Online	Citatio

Articles You May Be Interested In

Electron attachment dynamics following UV excitation of iodide-2-thiouracil complexes

J. Chem. Phys. (June 2022)

Photoelectron spectroscopic study of the negative ions of 4-thiouracil and 2,4-dithiouracil

J. Chem. Phys. (February 2011)

Insights into the dehydrogenation of 2-thiouracil induced by slow electrons: Comparison of 2-thiouracil and 1-methyl-2-thiouracil

J. Chem. Phys. (June 2018)

Challenge us.

What are your needs for periodic signal detection?



Find out more





Time-resolved photoelectron spectroscopy of iodide–4-thiouracil cluster: The $\pi\pi^*$ state as a doorway for electron attachment

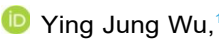
Cite as: J. Chem. Phys. 160, 054301 (2024); doi: 10.1063/5.0187557 Submitted: 14 November 2023 • Accepted: 9 January 2024 •







Published Online: 1 February 2024



Megan Asplund, 1 D Masafumi Koga, 1 D Ying Jung Wu, 1 D and Daniel M. Neumark 1.2.a. D





AFFILIATIONS

- Department of Chemistry, University of California, Berkeley, California 94720, USA
- Chemical Sciences Division, Lawrence Berkeley National Laboratory, Berkeley, California 94720, USA
- ^{a)}Author to whom correspondence should be addressed: dneumark@berkeley.edu

ABSTRACT

The photophysics of thiobases – nucleobases in which one or more oxygen atoms are replaced with sulfur atoms – vary greatly depending on the location of sulfonation. Not only are direct dynamics of a neutral thiobase impacted, but also the dynamics of excess electron accommodation. In this work, time-resolved photoelectron spectroscopy is used to measure binary anionic clusters of iodide and 4-thiouracil, I-4TU. We investigate charge transfer dynamics driven by excitation at 3.88 eV, corresponding to the lowest $\pi\pi^*$ transition of the thiouracil, and at 4.16 eV, near the cluster vertical detachment energy. The photoexcited state dynamics are probed by photoetachment with 1.55 and 3.14 eV pulses. Excitation at 3.88 eV leads to a signal from a valence-bound ion only, indicating a charge accommodation mechanism that does not involve a dipole-bound anion as an intermediate. Excitation at 4.16 eV rapidly gives rise to dipole-bound and valence-bound ion signals, with a second rise in the valence-bound signal corresponding to the decay of the dipole-bound signal. The dynamics associated with the low energy $\pi\pi^*$ excitation of 4-thiouracil provide a clear experimental proof for the importance of localized excitation and electron backfilling in halide-nucleobase clusters.

Published under an exclusive license by AIP Publishing. https://doi.org/10.1063/5.0187557

I. INTRODUCTION

The photophysics of natural nucleobases have been extensively studied owing to their biological significance and the role that fast non-adiabatic relaxation plays in their high photostability.¹⁻⁸ In contrast, single atom substitutions, such as the replacement of one or both nucleobase oxygens with sulfur atoms, have been shown to have profound impacts on relaxation pathways following photoexcitation.9-17 These nucleobase derivatives are of interest owing to their potential in pharmacological applications, such as phototherapy where they can act as photosensitizers.9-11,18,19 For example, upon photoexcitation of sulfur substituted nucleobases, the quantum yield for relaxation to the triplet manifold nears unity, resulting in increased reactivity compared to canonical nucleobases that undergo rapid relaxation to their ground electronic states. 7,9,11,14,17 It is also of interest to contrast the interactions of natural and thio-substituted nucleobases with low energy electrons since this interaction is also important in radiation chemistry and

biology. This latter consideration motivates the present study, which examines the dynamics of photoexcited I- 4-thiouracil (I- 4TU) cluster anions and builds on our previous work on $\ensuremath{\text{I}}\xspace \-$ 2-thiouracil (I-2TU) to elucidate the effects of sulfonation on charge transfer mechanisms.

Within a cell, DNA damage may occur via direct or indirect interactions between photons and a DNA strand. In particular, indirect interactions via low energy electrons have been implicated as a significant contributor to strand breakages. 20,21 These considerations have motivated electron scattering and photoionization studies of gas phase canonical and modified nucleobase species, 22 as the nucleobase is predicted to be the initial site of electron attachment.²³⁻²⁶ Dissociative electron attachment (DEA) measurements show that the major product of interactions of nucleobases and low energy (3 eV) electrons is the H loss from the base via NH bond ruptures.^{27–31} DEA studies of 2-thiouracil (2TU) similarly show that NH bond cleavage accounts for the majority of

dissociation products, $^{32-34}$ though equivalent results have not been published for 4-thiouracil.

Electron scattering experiments are complemented by photoelectron spectroscopy (PES) of nucleobase anions. These experiments demonstrate that during electron capture, a low energy electron may become associated with a nucleobase as either a dipolebound (DB) or valence-bound (VB) anion, which are readily distinguished by their spectroscopic signals.^{35–37} DB anions can only form for a molecule with a sufficiently large dipole moment, 38,39 as they are the result of association between an excess electron and a molecular dipole. DB anions are generally weakly bound, with a geometry very similar to the neutral. An excess electron can also be captured by one of the unoccupied valence (usually anti-bonding) orbitals of the molecule, forming a VB anion. In nucleobases, the VB anion forms by population of the π^* orbital, causing a ring puckering distortion of the molecule. 40,41 PES of uracil anions shows features from both DB and VB anions, with an intense, sharp feature at low binding energy, corresponding to a DB anion, as well as a broader feature associated with a rare tautomer valence

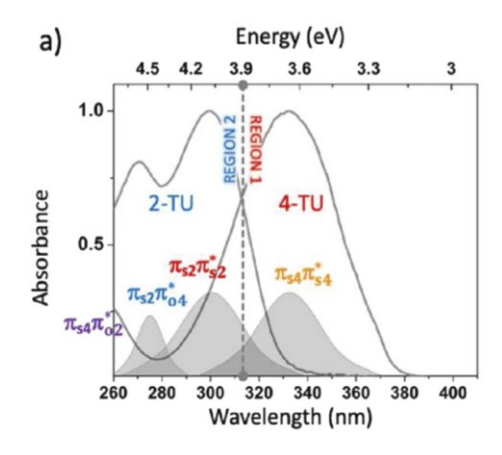
Photoelectron spectroscopy of the 4-thiouracil and dithiouracil anions by Bowen and co-workers, ⁴² supported by computational work, ⁴³ demonstrates that both thiobases can form stable valence-bound anions in their canonical forms. These data show no evidence for stable dipole-bound anions for either thiobase. However, DEA of 2TU implicates a DB state in facilitating dissociative electron attachment to the thiobase, ³² indicating the possible importance of transient DB anions in these systems.

The dynamics of electron capture have been investigated for several nucleobases by time-resolved photoelectron spectroscopy (TRPES)⁴¹ and one-photon photodepletion spectroscopy of iodide-nucleobase clusters.⁴⁴ In TRPES experiments, the halide anion acts as an electron donor, with charge transfer instigated

by a femtosecond UV pump pulse. The resultant transient negative ions of the nucleobase are probed by a second femtosecond laser pulse that detaches the excess electron. We have previously carried out experiments on iodide–nucleobase clusters, including iodide–uracil,⁴⁵⁻⁴⁷ iodide–thymine,^{47,48} iodide–adenine,⁴⁹ iodide–uracil H2O,^{50,51} and iodide–2-thiouracil,⁵² while photodepletion has been applied to clusters of iodide with all of the canonical DNA and RNA nucleobases,^{44,46,53} as well as iodide–2-thiouracil, iodide–4-thiouracil, and iodide–2,4-thiouracil.^{54,55}

In each of the systems measured by TRPES, the DB anion is formed when the cluster is excited near its vertical detachment energy (VDE, near 4 eV for these clusters), exciting the excess electron into a DB state of the complex. One also observes rapid formation of VB states upon near-VDE excitation, although direct excitation of an electron into the VB state is not generally favorable. In measurements where the cluster is excited near its VDE, the DB signal arises more quickly than the VB signal, suggesting that the DB state acts as a gateway state. However, the VB signal is also observed in experiments with higher energy excitation (4.7 eV) where there is no evidence of DB ion formation. Although we originally proposed that photoexcitation directly transferred an electron from I- into a VB state of the nucleobase, subsequent work suggested an alternate mechanism in which the UV pump pulse excites the strong $\pi\pi^*$ absorption of the nucleobase followed by electron transfer from the I⁻ into π vacancy. ⁴⁶ Thus far, however, direct experimental evidence for either mechanism has been elusive.

The cluster I⁻ 4TU offers an opportunity to examine how VB chromophore ions can form without the involvement of a DB state. As shown in Fig. 1, the isolated thiobase 4TU has a particularly low energy $\pi\pi^*$ excitation relative to other nucleobases, such as uracil or 2TU,¹⁷ and photodepletion measurements of the I⁻ 4TU cluster⁵⁵ show an electronic absorbance below the VDE of the cluster (Fig. 1, right panel). This presents an opportunity to isolate the



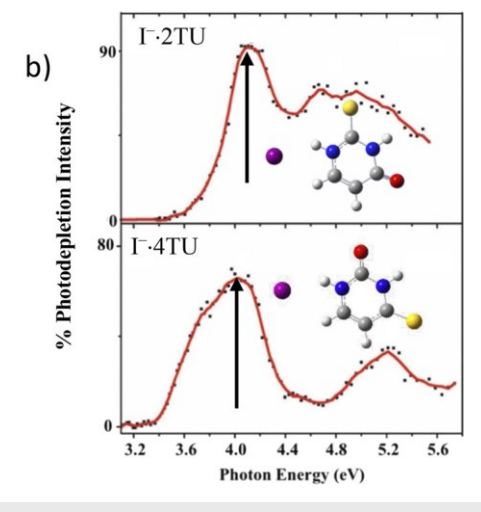


FIG. 1. (a) Absorption spectra of 2TU and 4TU in a carbon tetrachloride solution with bands assigned to specific $\pi\pi^*$ transitions adapted from the work of Mohamadzade *et al.*¹⁰ (b) Gas phase photodepletion spectra of I⁻ · 2TU and I⁻ · 4TU adapted from the work of Uleanya *et al.*⁴² with optimized geometries for both clusters and arrows representing the VDE of each cluster.

potential impact of $\pi\pi^*$ excitation while minimizing the contributions of higher energy electron scattering mechanisms. Additionally, as I $^-$ 4TU DB anions are easily distinguished from valence excitations by TRPES, a short-lived DB anion signal for the cluster can, in principle, be separated from the broad shoulder at \sim 3.8 eV observed by photodepletion spectroscopy.

In this study, we use TRPES of the iodide–4-thiouracil cluster to investigate its dynamics following excitation of a $\pi\pi^*$ transition below the cluster VDE, as well as higher energy excitation near the cluster VDE. Our results at the lower excitation energy isolate dynamics following $\pi\pi^*$ excitation, providing empirical evidence for the VB formation mechanism previously postulated wherein $\pi\pi^*$ chromophore localized excitation allows the excess electron to occupy a π orbital vacancy. This mechanism can proceed without a DB anion intermediate. At excitation near the cluster VDE, we confirm the existence of a transient DB state and characterize formation of the VB anion with two rise times, with the first caused by chromophore excitation and the second by the DB anion to VB anion conversion

II. METHODS

The TRPES setup has been described in other publications, ^{56,57} but a brief summary will be provided here. An inert carrier gas, in this case argon, flows over a reservoir of methyl iodide and through a cartridge containing the solid 4-thiouracil sample (97%, Alfa Aesar). An Even–Lavie pulsed valve heated to 220 °C and operating at 500 Hz generates a gas pulse that passes through an ionizing filament. Iodide anions are produced from dissociative electron attachment to CH₃I, which then cluster to gas phase 4-thiouracil to make the species of interest. Ions in the pulsed beam are extracted perpendicularly by using a Wiley McLaren time-of-flight mass spectrometer⁵⁸ that includes a mass gate to selectively pass iodide–4-thiouracil clusters.

In the interaction region, pump and probe laser pulses intersect with the cluster packets within a velocity-map imaging assembly. The photodetached electrons are detected by a pair of chevron-stacked microchannel plates coupled to a phosphor screen. The phosphor screen is read by a CCD camera, and the raw data images

are processed using BASEX⁵⁹ to generate the kinetic energy spectra and angular distributions of the photoelectrons.

Laser pulses are generated by using a KM Griffin Oscillator and KM Dragon Amplifier, producing-2 mJ/pulse at 1000 Hz repetition rate, with the fundamental centered at 1.55 eV and a pulse duration of 35 fs. To generate the pump pulse, a portion of this output is directed into a TOPAS-C optical parametric amplifier to generate tunable visible light that is subsequently doubled by a BBO crystal to obtain the final UV excitation wavelength. The remainder of the laser pulse serves as the probe (detachment) pulse. It can be directed into a delay stage and used to trace the time evolution of transient anion species of the chromophore. Alternatively, it can be frequency doubled by a BBO and the subsequent 3.14 eV probe pulse can photodetach free atomic I-, one of the major dissociation products for the cluster. The cross-correlation of the pump and probe pulses sets the instrumental response time at about 80 fs.

Dissociation of the I $^-$ 4TU cluster to I $^-$ and 4TU was investigated theoretically using the Gaussian 16 computing package 60 at the MP2 level of theory with an augmented Dunning basis set aug-cc-pVDZ for C, H, O, and N and an additional set of diffuse functions (aug-cc-pVDZ-pp) for I. 61

III. RESULTS

Figure 2 shows one color photoelectron spectra collected at hu = 3.88 and 4.92 eV, just under and well above the expected cluster VDE of 4 eV based on photodepletion spectroscopy. The most intense feature of the spectrum at 4.92 eV excitation is a peak centered at an electron kinetic energy (eKE) of 0.74 eV or a binding energy of 4.18 eV, with binding energy defined as eB£ hu-eKE. Based on previous work on related systems, this feature is assigned to direct detachment to the I($^{\circ}$ P3/2)·4TU spin-orbit state of the neutral cluster, yielding VDE = 4.18 eV for I · 4TU. This value is close to the calculated VDE for I · 4TU from the work of Uleanya and Dessent (4.32 eV), as well as experimental VDE values for iodide—thymine, iodide—uracil, and iodide—thiouracil clusters determined by photoelectron spectroscopy. 11,45,47,48,52 A

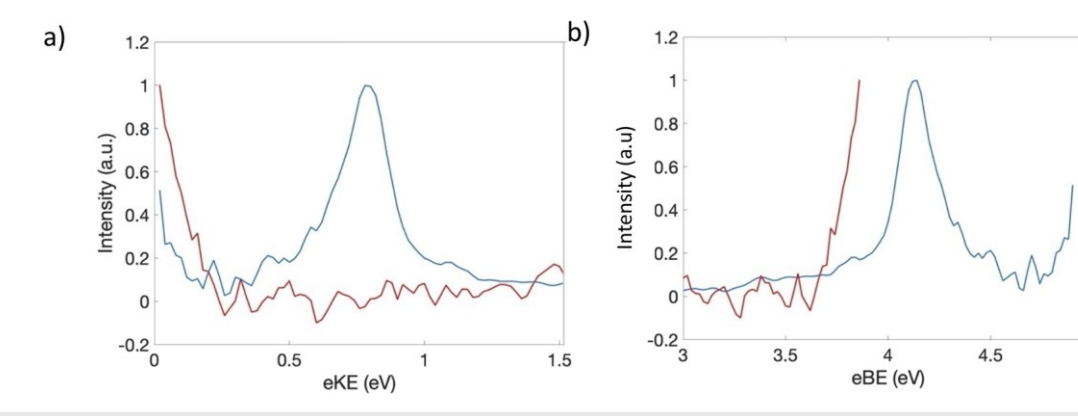


FIG. 2. One color spectra of I⁻ · 4TU collected with 4.92 eV (blue) and 3.88 eV (red) excitation plotted in electron kinetic energy [eKE, (a)] and electron binding energy [eBE, (b)].

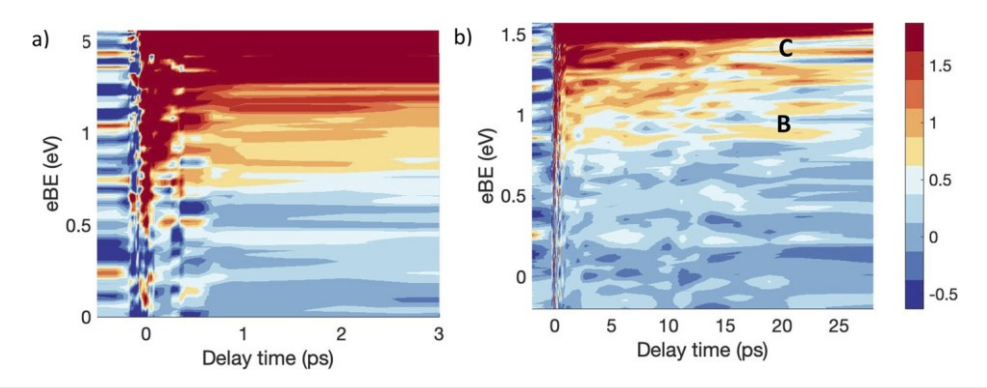


FIG. 3. Contour plot of I⁻ ⋅ 4TU TRPE spectra with 3.88 eV pump and 1.55 eV probe pulses at shorter (a) and longer (b) delay times.

second, less intense feature is seen near 0 eKE and corresponds to resonant excitation of the cluster followed by electron autodetachment (AD), as previously determined for similar clusters. 47,48,51

The spectrum collected at 3.88 eV excitation has a single feature at low eKE. This excitation is below the VDE of the cluster, so the signal is due to AD or direct detachment below the VDE.

Figure 3 shows contour plots of time-resolved photoelectron spectra at shorter (a) and longer (b) pump-probe delays at a pump photon energy of 3.88 eV, corresponding to the low energy $\pi\pi^*$ excitation of the chromophore, and a 1.55 eV probe pulse. There are two primary features apparent in Fig. 3. The first, labeled feature C in the right panel, is very intense and occurs mainly between 1.5 and 1.55 eBE, corresponding to near-zero (0–0.05 eV) kinetic energies. This is the energy range expected for AD, and it appears that this signal is enhanced at positive pump-probe delays. The spectra also show a broad feature B from 0.8 to 1.4 eV, which corresponds well with the VDE of the 4TU valence-bound ion as measured by one photon photoelectron spectroscopy by Li *et al.* (0.7–1.5 eV). The feature arises very quickly after to before losing most of its intensity within a few hundred femtoseconds.

Figure 4 shows the analogous contour plots of TRPES measurements taken with 4.16 eV (near VDE) excitation and 1.55 eV probe and exhibits three distinct features. Near to, two of these features look quite similar to features B and C in Fig. 3 and are labeled accordingly. Notably, feature B is much longer lived in these spectra than the spectra with 3.88 eV excitation. The third feature in Fig. 4, feature A, is distinct from any feature in Fig. 3. It covers 0–0.3 eV and has a much narrower spectral profile than feature B. In previous measurements of iodide-chromophore clusters, features similar to feature A have been ubiquitous in near-VDE excitation measurements. 41,46,49–51,62 Based on its narrow shape and low binding energy, feature A can be labeled as the signal from a transient dipole-bound anion.

Dynamics at both excitation energies were also probed at 3.14 eV. This energy is sufficient to just detach bare I⁻ to neutral iodine. Figure 5 shows the contour plots of measurements with a 3.14 eV probe pulse and 3.88 eV (a) or 4.16 eV (b) pump pulses. The spectra are dominated by a single feature (D) at eBE \pm 3.06 eV, the electron affinity of atomic iodine. Feature D corresponds to photodetachment of the iodide fragment following dissociation of the photoexcited cluster to I⁻+ 4TU and has been seen in our previous studies of iodide–nucleobase complexes. 41,46,50,51

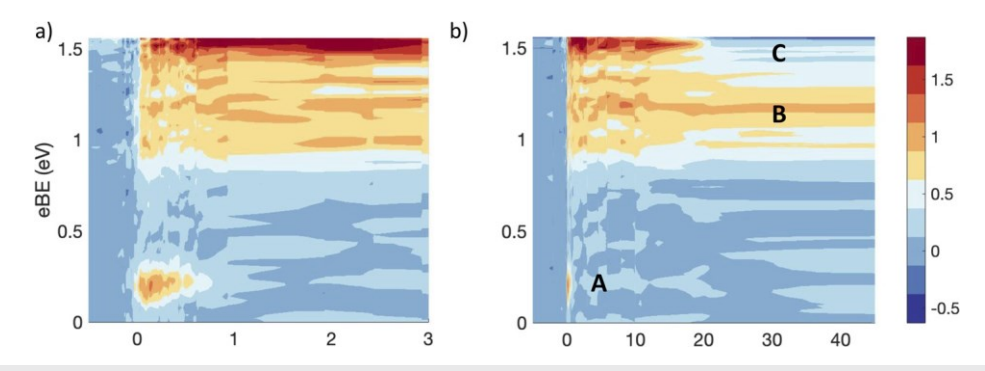


FIG. 4. Contour plot of I - 4TU TRPE spectra with 4.16 eV pump and 1.55 eV probe pulses at shorter (a) and longer (b) delay times.

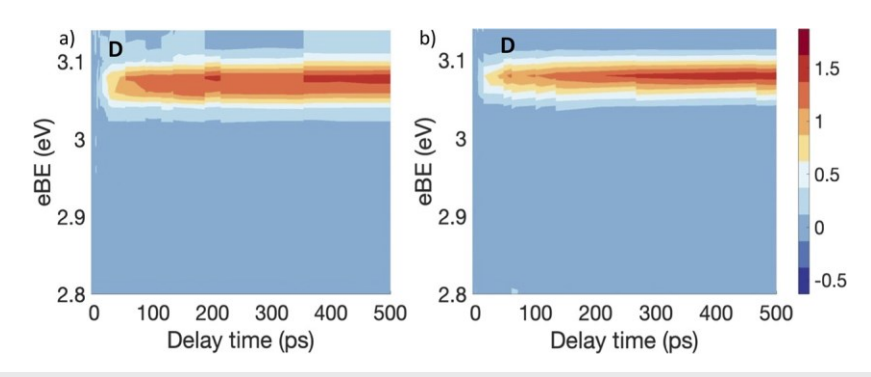


FIG. 5. Contour plot of I - · 4TU TRPE spectra with 3.88 eV (a) and 4.16 eV (b) pump and 3.14 eV probe pulses.

IV. ANALYSIS

The dynamics of this system are analyzed by integrating over features of the acquired spectra and then fitting the integrations to a convolution of a Gaussian experimental response function and a sum of exponential functions,

$$\begin{cases}
1 & \sqrt{-1} \\
I & t
\end{cases} = \frac{1}{\sigma_{CC}} \frac{1}{2\pi} \exp\left(-\frac{t^2}{2\sigma_{CC}^2}\right) \cdot \begin{cases}
I_0, & t < 0, \\
I & +\sum A \exp\left(-\frac{t}{T_0}\right) + c, & t \ge 0. \\
0 & i & \tau_i
\end{cases}$$
(1)

In this equation, I_0 is a constant offset from the background signal, σ_{CC} is the experimental response time of 80 fs, c is the

signal offset at very long time delays, and T_i are the intensity and time constant for the i-th exponential function. The time evolution for several of these signals requires multiple exponential terms to adequately fit the integrated plot. The integrated normalized intensities of features from the spectra collected with 3.88 eV excitation and 1.55 eV probe are plotted in Fig. 6 with the corresponding parameters for Eq. (1) reported in Table I. Integrated normalized intensities of features collected with 4.16 eV excitation and 1.55 eV probe are plotted in Fig. 7 with fitting parameters reported in Table II. In Figs. 6 and 7, data are indicated by open circles and the fits by solid lines.

In Fig. 6(a), the signal from feature B rises within the experimental resolution of 80 fs and decays biexponentially, with 80%

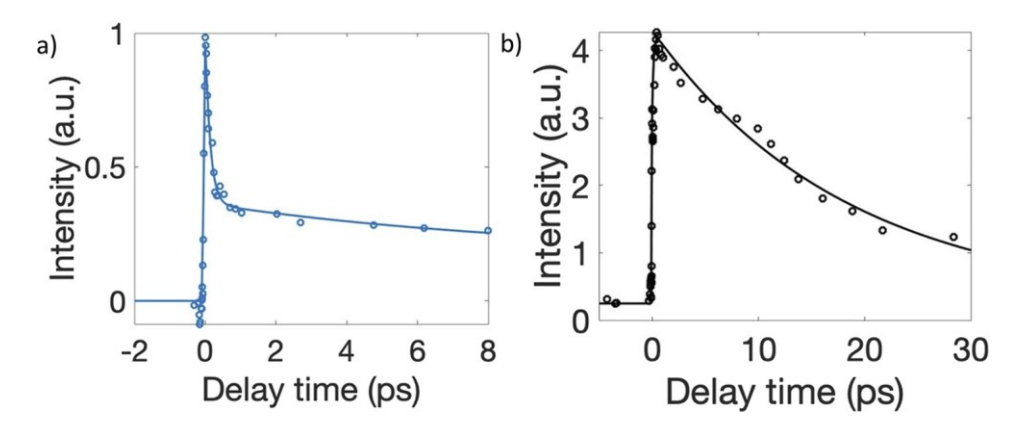


FIG. 6. Time evolution of integrated features B [blue, VB, (a)] and C [black, AD, (b)] for 3.88 eV excitation, 1.55 eV probe. Signals are scaled from raw data to normalize the maximum intensity of feature B to 1.

TABLE I. Fit parameters that reproduce the time evolution in Fig. 6.

	eBE (eV)	τι decay (fs)	τ₂ rise (fs)	τ₃ decay (ps)	A_1	A_2	Аз	С
Feature C	1.50-1.55		218 ± 93	18.4 ± 2.3	2	-0.51	1.0	• • • •
Feature B	0.7 - 1.2	139 ± 36		9.4 ± 4.7	0.81		0.19	0.17

^a All amplitudes shown here are normalized by the sum of the exponential amplitudes.

20

40

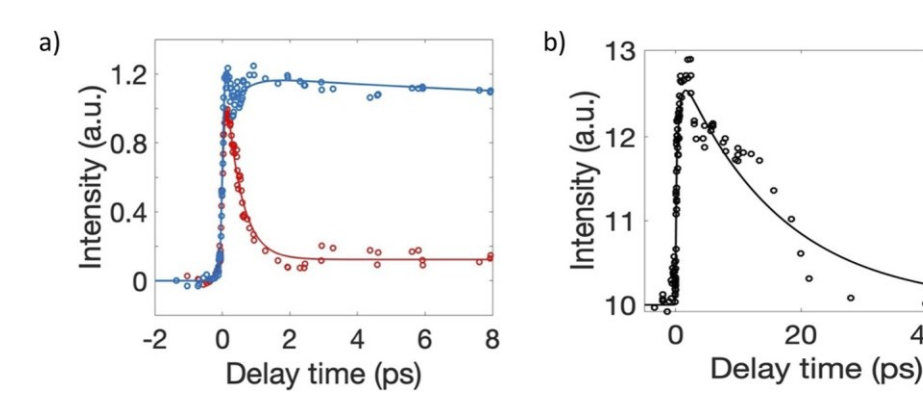


FIG. 7. Time evolution of integrated feature A (red, DB), feature B signal (blue, VB), and feature C (black, AD) for 4.16 eV excitation, 1.55 eV probe spectra. (a) Features A and B are normalized to maximum values of 1 and 1.2, respectively. (b) Feature C is scaled using the normalization factors for feature A.

TABLE II. Fit parameters that reproduce the time evolution in Fig. 7.

	eBE (eV)	τı (fs) decay	τ₂ (fs) rise	τ ₃ (ps) decay	A_1	A_2	<i>A</i> 3	С
Feature B	1.50–1.55 0.7–1.2 0–0.30	47.4 ± 6.3 442 ± 50	560 ± 390 442a	16.2 ± 3.8 13.1 ± 9.9	0.96 ^b	-0.51 -0.07	1.0 0.04	0.83

^aValue fixed using the decay of the DB signal.

of the signal decaying in τ_1 = 140 fs and an additional fraction decaying with τ_2 = 9.4 ps. At later times, the signal reaches an asymptotic value with a significant offset. The signal from feature C rises within about $\tau_2 = 200$ fs and then exhibits single exponential decay with $\tau_0 = 18.4 \text{ ps.}$

Figure 7 shows the temporal evolution of the three features seen in Fig. 4. In Fig. 7(a), feature A (red, DB anion) rises within the experimental resolution before undergoing single exponential decay with τ₁ 440 fs. A small signal offset remains at long time delays attributed to background noise. The signal from feature B (blue, VB anion) requires three time constants to fit accurately. The signal rises within instrument resolution, decays partially (with time constant τ_1), undergoes a second rise (τ_2), and then decays slowly (τ₃) before reaching an asymptotic offset. Qualitative examination of Fig. 7, as well as known mechanisms for DB state mediated VB ion formation, 30,45,52,64,65 suggests that depletion of the DB ion gives rise to the VB ion as the former state transitions into the latter. Accordingly, the rise τ_2 for the VB signal should be roughly equal to decay τ_1 for the DB signal. With three variable time constants, the precision of the fit is unacceptably low. If we fix τ_2 for the VB signal to 440 fs, i.e., τ_1 for feature A, we retrieve 47 fs for the initial VB decay constant τ_1 . The signal continues to decay with $\tau_3 = 13.1 \text{ ps.}$

Feature C in Fig. 7(b) has a rise time of $\tau_2 = 560$ fs and decays with $\tau_3 = 16.2$ ps. The fit for the AD signal is not as good as for the DB and VB signal, likely because of the narrow energy window for the integration, which is selected to minimize overlap with the VB feature.

The VDE of the DB ion shifts noticeably over the first picosecond following excitation. This can be better quantified by fitting feature C to a Gaussian function at each delay time and plotting the binding energy of the Gaussian peak over time, as shown in Fig. 8. Because of the rapid decay of the DB state, these values can be extracted only for the first 1-2 ps following excitation but over this time interval, the VDE of the DB state increases by about 50 meV, following a trend observed in the DB VDE values observed for I- ·U and $I^- \cdot U \cdot H_2O.45,51$

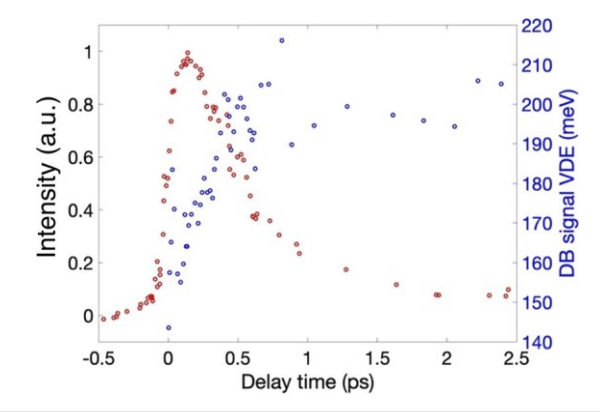


FIG. 8. Vertical detachment energies (blue) and normalized signal intensity for feature A (red, dipole-bound ion) up to 2.5 ps.

^bAll amplitudes shown here are normalized by the sum of the decay amplitudes.

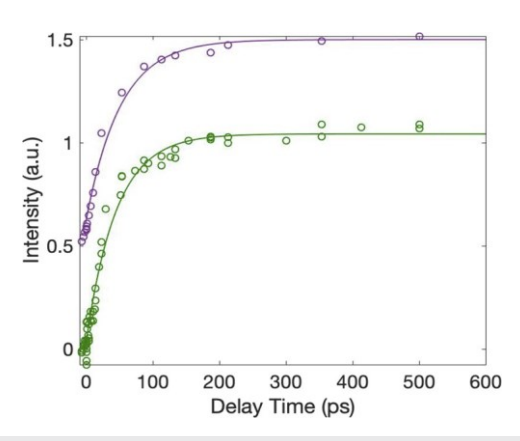


FIG. 9. Time evolution of normalized, integrated feature D for 4.16 eV (green) or 3.88 eV (purple) excitation and 3.14 eV probe spectra. The plot at 3.88 eV is offset vertically by 0.5 a.u. to improve readability.

Figure 9 shows the integrated signal from feature D for both excitation energies probed at 3.14 eV. The rise of the feature is slow enough that the Gaussian term is unnecessary, and the data can be fit using a simple exponential rise and intensity offset, as in the following equation;

$$I(t) = \begin{cases} 0, & t < 0, \\ I_{off} + A_i \exp\left(\frac{-t}{\tau_i}\right), & t \ge 0. \end{cases}$$
 (2)

The rise time for the I- signal at each excitation energy is given in Table III, as well as corresponding times measured for I-2-thiouracil (I- 2TU). Higher energy excitation corresponds to a slightly faster dissociation, with 3.88 and 4.16 eV excitation resulting in rise times of 56 and 41 ps, respectively. For near-VDE excitation at 4.16 eV, the I⁻ rise time for I \rightarrow 4TU is a factor of 3 longer than that of I \rightarrow 2TU

We have previously used Rice-Ramsperger-Kassel-Marcus (RRKM) theory 66,67 to model the dissociation of I- N to I+ N for various iodide nucleobase clusters, where N is the nucleobase. 46,50,51 The energy and vibrational frequencies of the I-4TU cluster were calculated at the MP2/aug-cc-pVDZ level, and the sum and density of states are determined by the Beyer-Swinehart direct count algorithm with the Stein-Rabinovitch modification. 68,69 As the transition state is loose, the reaction rate is determined variationally by modifying the iodine-nitrogen (N1) distance to find the lowest calculated rate constant. With the low frequency in-plane rocking and

TABLE III. Timescales describing the rise time of feature D for different clusters and excitation energies

I-	· 4TU	I− · 2TU		
hν (eV)	τ (ps)	hv (eV)	τ (ps)	
3.88 4.16	56.2 ± 9.4 48.9 ± 7.6	4.16	13.9 ± 1.6	
		4.74	9.0 ± 1.2	

out-of-plane twisting modes treated as hindered internal rotors, as described in greater detail elsewhere, 46,52 we calculate dissociation time constants of 17.0 ps with 3.88 eV excitation and 11.5 ps with 4.16 eV excitation at the bond dissociation energy of 1.04 eV found using the level of theory given in Sec. II. The dependence of these values on small changes in the bond dissociation energy is discussed in Sec. V.

V. DISCUSSION

The results obtained provide several interesting insights into the general set of thiouracils and previously measured iodide-nucleobase clusters.

A. VB formation by 3.88 eV excitation

Excitation at 3.88 eV corresponds to a localized $\pi\pi^*$ transition of 4TU but lies below the VDE of the I^{-} 4TU cluster of 4.18 eV as determined by our photoelectron spectrum. Spectra show no evidence for DB state formation, so such a state is not acting as a gateway to the observed VB anion state.

Previous iodide-nucleobase measurements have similarly resulted in spectra with the VB signal but not DB signal, but these were all taken at excitation energies at 4.5–4.7 eV, well above the cluster VDE. 41,45,50 It was postulated, primarily based on computational results, that VB anions were formed by chromophorelocalized $\pi\pi^*$ excitation followed by electron transfer from the halide to the hole in the chromophore π orbital, as shown in the following equation with N as the nucleobase:46

$$I^{-} \cdot N(\pi^{4}\pi^{*0}) \xrightarrow{h l^{pum}} I^{-} \rightarrow I^{-} \cdot N(\pi^{3}\pi^{*1}) \rightarrow I \cdot N(\pi^{4}\pi^{*1}).$$
 (3)

However, due to the high energy excitation, indirect electron scattering mechanisms involving capture of a photodetached electron from the I⁻ into the π^* orbital, leading to the same final state, could not be ruled out.

The experimental results here provide strong empirical evidence for the $\pi\pi^*$ excitation scheme in Eq. (3). The generation of a π orbital vacancy makes charge transfer to the thiobase energetically favorable even at excitation below the cluster VDE. Our results further indicate that this process is sufficiently rapid to account for the IRF limited (sub 80 fs) VB signal rise not only in this system but also in the previous above VDE excitation energy measurements in

The rapid disappearance of this signal ($\tau_1 = 140 \text{ fs}$) is attributed to back electron transfer (BET) that results in reformation of iodide, as in previous studies of similar clusters [Eq. (4a)]. 41,46,51,52,70 BET becomes less favorable if the iodine moves away from the valencebound anion, a reasonable expectation given that the iodine/VB anion interaction potential will be quite different from the ground state I-4TU potential. Once the I atom moves away, AD can become the primary decay mechanism [Eq. (4b)],

$$I \cdot 4TU_{\overline{VB}} \xrightarrow{BET} I^- \cdot 4TU,$$
 (4a)

$$I \cdot 4TU_{\overline{V}B} \rightarrow I \cdots 4TU_{\overline{V}B} \xrightarrow{AD} I + 4TU + e^{-}.$$
 (4b)

The slower time constant, 77 9 ps, is then attributed to this latter process.

B. VB and DB dynamics with 4.16 eV excitation

Excitation of the cluster at 4.16 eV, near the experimentally determined VDE, results in both DB and VB transient anion signals, as we have seen in previous iodide–nucleobase measurements. $^{41,45,47-50,62}$ The presence of the DB anion of 4TU is notable, as photoelectron spectroscopy of 4TU $^{-42}$ and photodepletion spectroscopy of I $^-\cdot$ 4TU 55 did not detect this dipole-bound species.

The DB signal of $I^- \cdot 4TU$ decays in 440 fs, whereas measurements of the $I^- \cdot 2TU$ cluster show the DB signal that rises and almost entirely decays within the instrument response time. This is a rather significant change in dynamics due to thionation position, with the conversion for $I^- \cdot 2TU$ remaining anomalously rapid compared to $I^- \cdot U$, $I^- \cdot 4TU$, and $I^- \cdot U \cdot H \cdot D$. It suggests that geometric concerns or the nearly degenerate $\pi\pi^*$ excitations of neutral 2TU play a role in its unusual dynamics that bears further investigation.

The DB signal decays almost entirely within 2 ps, with a negligible signal offset at longer time delay. This result is similar to dynamics observed for I $^-$ 2TU and I $^-$ CH₃NO₂, in which conversion from DB to VB is relatively complete. By comparison, the DB signal from near-VDE excited I $^-$ U and I $^-$ U·H₂O clusters exhibits a bi-exponential decay, with a large portion of the signal remaining after several ps. The complete DB to VB conversion of the I $^-$ 4TU, I $^-$ 2TU, and I $^-$ CH₃NO₂ clusters is consistent with a VB state lower in energy than the DB state. ^{35,43,71}

The VDE of the DB signal demonstrates a shift to higher binding energy over the first 1–2 ps following excitation (Fig. 8). This shift has been attributed to motion of the neutral iodine, as the increased distance between iodine and the DB anion reduces volume exclusion effects that destabilize the DB state at the shortest pump/probe delay times. 45,51 Comparable measurements in I $^-$.U and I $^-$.U ·H2O have shown that the VDE reaches an asymptote in 15–20 ps that agrees with that of the bare DB anion, suggesting

that the iodine has fully dissociated from the cluster. Owing to the short-lived DB anion of I^- 4TU, we are unable to fully replicate this measurement. However, the VDE shifts in the first 1–2 ps suggest that initial iodine motion in I^- 4TU is similar to the other clusters.

For the VB signal formed by 4.16 eV excitation, an initial rise is seen within the experimental response time, followed by rapid decay (\dagger) and then a second signal rise (\dagger). The two distinct rise features indicate two VB formation mechanisms. The initial, IRF-limited rise can be attributed to the same mechanism underlying VB signal appearance with 3.88 eV excitation; the $\pi\pi^*$ excitation is accessible with a 4.16 eV pump pulse, allowing for prompt transfer of the excess iodide electron to the π orbital vacancy. The second rise time τ_2 for the VB state can be fit well using the decay time for the DB state, indicating DB to VB conversion. The second rise τ_2 is absent for the VB signal under 3.88 eV excitation, given that no DB population is formed. With 4.16 eV excitation, however, we are able to see both VB formation mechanisms contributing to the overall signal level.

The VB signal offset observed at long time delays is consistent with the calculated stability of the VB state of $4TU^-$ and its measurement as a photoproduct of I $^-$ 4TU in previous work. The VB signal generated at 4.16 eV retains most of its strength after 10 ps, in contrast to the VB signal from 3.88 eV excitation. This can be justified by considering the two VB formation mechanisms active at the higher excitation energy. The initial population of VB anions is

depleted by rapid back electron transfer for both excitation energies, represented by decay constant τ_1 . Only for near-VDE excitation does DB to VB formation contribute to VB signal strength after nearly 500 fs. As discussed above, the DB VDE shifts noticeably within this time frame, indicating that iodine has moved from its initial position in the anion ground state. This inhibits back electron transfer compared to the initial cluster geometry, with bond-lengthened clusters likelier to undergo AD. Moreover, AD is the only possible decay mechanism once the I atom fully leaves the cluster.

C. Autodetachment dynamics

Autodetachment of the excess electron is apparent in the one color spectra in Fig. 2 at both excitation energies. In previous time-resolved measurements of I $^-$ U and I $^-$ T, the AD signal exhibited a distinct depletion around to, as the probe pulse detaches transients that would otherwise undergo AD. ⁴⁸ In I $^-$ 4TU, as in I $^-$ U H₂O, ⁵⁰ the depletion is not obvious, suggesting a VB state that is stabilized relative to AD.

Instead, the time-resolved spectra in Figs. 3 and 4 show significant enhancement of a low eKE signal at positive time delays up to 20 ps, "overshooting" the baseline level established at negative time delays. This suggests that the 1.55 eV pulse is not purely acting as a probe pulse, but produces a new state that can decay by AD. The AD signal rise lags behind that of the VB by a few hundred femtoseconds, indicating that the new state may be an excitation of the VB anion, as shown in the following equation:

$$I \cdot 4TU_{\overline{VB}} \xrightarrow{\underline{h} V^{p^{r}}} \xrightarrow{obe} [I \cdot 4TU_{\overline{B}}]^{*} \xrightarrow{AD} I \cdot 4TU + e^{-}.$$
 (5)

The existence of a higher-lying VB excited state was previously postulated based on measurements of 1 . Of H $_{\odot}$ and

 $I^- \cdot U_{-}^{48}$ clusters which also show significant overshoot at positive time delays. However, $I^- T$, which exhibits rapid, nearly monoexponential decay of the VB state, lacks this AD enhancement. The strongest predictor of the AD overshoot seems to be a VB anion signal that lasts longer than ~ 5 ps, further strengthening the assignment of feature C to AD from an excited VB state.

The AD signal enhancement decays with time constants of $\sim\!\!18$ and $\sim\!\!16$ ps for 3.88 and 4.16 eV excitation, respectively. For $1^-\cdot U$ and $1^-\cdot U\cdot H_2O$, the intensity of the AD signal mirrors the decay of population of the VB state. 48,50 This does not appear to be true for the 1^- 4TU cluster. In particular, a very large fraction of the VB signal remains at 100 ps in the case of 4.16 eV excitation due to the stability of the VB anion, whereas the AD signal enhancement decays entirely. This discrepancy may arise from dynamics in the cluster

that impact the accessibility of the 4TU*_{VB} state but do not significantly alter the VB state itself, such as a change to solvation effects from neutral iodine motion.

D. Decay products

Photofragment product spectroscopy performed by Uleanya *et al.* indicates that I⁻ 4TU clusters excited at 4 eV produce atomic I⁻ as a major photofragment and the deprotonated thiobase [4TU-H]⁻ as a very minor photofragment.⁵⁵ Dissociation of I⁻ is directly measured in our setup with the 3.14 eV probe pulse, which shows a signal rising mono-exponentially with time constants of 56 ps for the 3.88 eV pump energy and 41 ps for the 4.16 eV pump

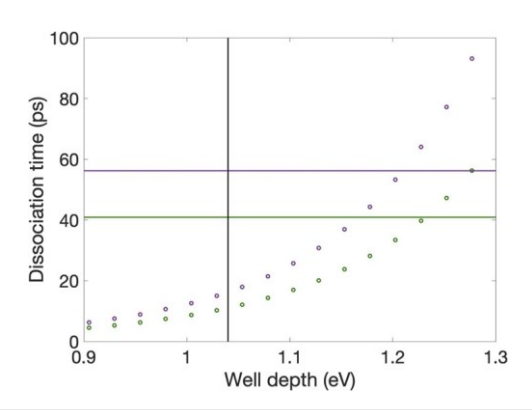


FIG. 10. RRKM calculated dissociation time vs dissociation potential well depth for 3.88 eV (purple) and 4.16 eV (green) excitation. Experimental dissociation time constants are plotted as horizontal lines and the calculated depth given by the vertical line at 1.04 eV.

energy. Iodide may be reformed by back electron transfer [Eq. (4a)] followed by dissociation of the vibrationally excited cluster, as shown in Eq. (6)

$$I \cdot 4TU_{VB} \xrightarrow{BET} I^- \cdot 4TU \rightarrow I^- + 4TU.$$
 (6)

As discussed in Sec. IV, the experimental dissociation times are nearly four times larger than those calculated by RRKM using the calculated bond dissociation energy of 1.04 eV. The calculated dissociation time of the I $^-$ ·2TU cluster, by contrast, is in good agreement with the experimental value. 52

While one might attribute this discrepancy to a mechanistic difference between I^-4TU and I^-2TU , the results of the RRKM calculation are highly dependent on the energy difference between the reactant and the calculated transition state. Figure 10 shows cluster dissociation time constants for I- · 4TU associated with different potential well depths with all other parameters equal. The well depth itself is a calculated value involving a loose, barrierless transition state and therefore somewhat uncertain. Increasing the well depth by about 15% results in a calculated time constant that agrees with the experimentally determined I- rise time. Alternatively, the well depth can be approximated from experimental values as the difference between the cluster VDE and the electron affinity of atomic I, or 4.18–3.06 eV ≠1.12 eV. Even this correction would be sufficient to bring the RRKM calculation dissociation time within a factor of 2 of the experimental value. It is therefore likely that the discrepancy between calculated and experimental dissociation times in I-4TU is caused by uncertainty of the well depth and that the same mechanism for I⁻ production, Eq. (6), holds for I⁻ · 4TU and $I^- \cdot 2TU$.

VI. CONCLUSION

TRPES has been used to examine charge transfer dynamics of the I⁻ 4TU binary cluster. Excitation at 3.88 eV gives rise to a VB signal without the mediation of a DB "gateway state." Rather, a localized $\pi\pi^*$ excitation of the chromophore allows for electron transfer to a vacancy in an energetically accessible π orbital of 4TU. The low

energy $\pi\pi^*$ excitation of 4TU rules out other mechanistic possibilities, vindicating this pathway as a method of transient formation. Excitation at 4.16 eV leads to both VB and DB signals, with the transition between DB and VB states clear in the spectra taken with 1.55 eV probe.

At both excitation energies, the VB state decays by rapid back-electron transfer to the I atom and a slower process attributed to AD. In addition, at positive pump–probe delays, we observe an enhanced slow photoelectron signal attributed to probe-pulse excitation (1.55 eV) of the VB state to a higher-lying state that undergoes AD. Finally, with the 3.14 eV probe pulse, we find that dissociation to I $_+$ 4TU occurs on a time scale of 10 s of ps. This channel is attributed to back-electron transfer to form vibrationally excited I $_-$ 4TU followed by statistical ground state dissociation.

This work shows that there are distinct differences in the dynamics of photoexcited I $^-$ 4TU compared to I $^-$ 2TU and iodide complexes with the canonical nucleobases. The most important of these arises owing to the presence of a $\pi\pi^*$ transition below the cluster VDE in I $^-$ 4TU. It will be of considerable interest to see if the dynamics of iodide complexed with 2,4-dithiouracil (I $^-$ 2, 4TU) lie closer to those of I $^-$ 4TU or I $^-$ 2TU; these studies are currently under way in our laboratory.

ACKNOWLEDGMENTS

This research was supported by the National Science Foundation under Grant No. CHE-2154629 and by CALSOLV, the Center for Solvation Studies at the University of California, Berkeley. M.K. acknowledges the support from the Japan Society for the Promotion of Science (JSPS) Overseas Research Fellowships.

AUTHOR DECLARATIONS

Conflict of Interest

The authors have no conflicts to disclose.

Author Contributions

Megan Asplund: Conceptualization (equal); Data curation (equal); Formal analysis (equal); Visualization (equal); Writing – original draft (equal); Writing – review & editing (equal). Masafumi Koga: Formal analysis (supporting); Writing – review & editing (equal). Ying Jung Wu: Formal analysis (supporting); Investigation (supporting); Writing – review & editing (supporting). Daniel M. Neumark: Conceptualization (equal); Funding acquisition (equal); Methodology (equal); Supervision (equal); Writing – review & editing (equal).

DATA AVAILABILITY

The data that support the findings of this study are available from the corresponding author upon reasonable request.

REFERENCES

- ¹S. Matsika, J. Phys. Chem. A **108**, 7584–7590 (2004).
- ²C. E. Crespo-Hernández, B. Cohen, P. M. Hare, and B. Kohler, Chem. Rev. **104**, 1977–2020 (2004).
- ³A. Stolow, A. E. Bragg, and D. M. Neumark, Chem. Rev. **104**(4), 1719–1758 (2004).
- ⁴C. T. Middleton, K. de La Harpe, C. Su, Y. K. Law, C. E. Crespo-Hernández, and B. Kohler, Annu. Rev. Phys. Chem. **60**, 217–239 (2009).
- ⁵M. Barbatti, A. J. A. Aquino, J. J. Szymczak, D. Nachtigallová et al., Proc. Natl. Acad. Sci. U. S. A. 107(50), 21453–21458 (2010).
- ⁶R. Improta, F. Santoro, and L. Blancafort, Chem. Rev. **116**(6), 3540–3593 (2016).
- ⁷H. Yu, J. A. Sánchez-Rodríguez, M. Pollum, E. Crespo-Hernandez, S. Mai, P. Marquetand, L. Gonzalez, and S. Ullrich, Phys. Chem. Chem. Phys. **18**, 20168–20176 (2016).
- ⁸L. Martínez-Fernández, G. Granucci, M. Pollum, C. E. Crespo-Hernandez, M. Persico, and I. Corral, Chem. A Eur. J., 23(11), 2619–2627 (2017).
- ⁹M. Pollum, S. Jockusch, and C. E. Crespo-Hernandez, J. Am. Chem. Soc. **136**, 17930–17933 (2014).
- ¹⁰M. Pollum and C. E. Crespo-Hernández, J. Chem. Phys. **140**, 071101 (2014).
- ¹¹M. Pollum, S. Jockusch, and C. E. Crespo-Hernandez, Phys. Chem. Chem. Phys. 17, 27851–27861 (2015).
- ¹² S. Mai, P. Marquetand, and L. González, J. Phys. Chem. Lett. 7(11), 1978–1983 (2016).
- ¹³ S. Mai, M. Pollum, L. Martínez-Fernández, N. Dunn, P. Marquetand, I. Corral, C. E. Crespo-Hernández, and L. González, Nat. Commun. 7, 13077 (2016).
- ¹⁴ J. A. Sánchez-Rodríguez, A. Mohamadzade, S. Mai, B. Ashwood, M. Pollum, P. Marquetand, L. González, C. E. Crespo-Hernández, and S. Ullrich, Phys. Chem. Chem. Phys. 19(30), 19756–19766 (2017).
- ¹⁵ A. Mohamadzade, S. Bai, M. Barbatti, and S. Ullrich, Chem. Phys. **515**, 572–579 (2018).
- ¹⁶ S. Ullrich, Y. Qu, A. Mohamadzade, and S. Shrestha, J. Phys. Chem. A **126**(44), 8211–8217 (2022).
- ¹⁷ A. Mohamadzade, A. Nenov, M. Garavelli, I. Conti, and S. Ullrich, J. Am. Chem. Soc. **145**, 11945–11958 (2023).
- ¹⁸ L. A. Ortiz-Rodriguez and C. E. Crespo-Hernández, Chem. Sci. 11, 11113–11123 (2020).
- ¹⁹V.-H. Nguyen, S. Heo, C. W. Koh, J. Ha, G. Kim, S. Park, and Y. Yoon, ACS Sens. 6(9), 3462–2467 (2021).
- ²⁰B. Boudaïffa, P. Cloutier, D. Hunting, M. A. Huels, and L. Sanche, Science **287**, 1658–1660 (2000).
- ²¹S. J. Jishnu Narayanan, D. Tripathi, P. Verma, A. Adhikary, and A. K. Dutta, ACS Omega 8(12), 10669–10689 (2023).
- ²²M. S. Robinson, M. Niebuhr, and M. Gühr, Molecules **28**, 2354 (2023).
- ²³R. Barrios, P. Skurski, and J. Simons, J. Phys. Chem. B **106**, 7991–7994 (2002).
- ²⁴J. Berdys, I. Anusiewicz, P. Skurski, and J. Simons, J. Am. Chem. Soc. 126, 6441–6447 (2004).
- ²⁵ F. Martin, P. D. Burrow, Z. L. Cai, P. Cloutier, D. Hunting, and L. Sanche, Phys. Rev. Lett. **93**, 068101 (2004).
- ²⁶J. Simons, Acc. Chem. Res. **39**, 772–779 (2006).
- ²⁷G. Hanel, B. Gstir, S. Denifl, P. Scheier, M. Probst, B. Farizon, M. Farizon, E. Illenberger, and T. D. Märk, Phys. Rev. Lett. **90**(18), 188104 (2003).
- ²⁸S. Denifl, S. Ptasinska, M. Cingel, S. Matejcik, P. Scheier, and T. D. Märk, Chem. Phys. Lett. **377**, 74–80 (2003).
- ²⁹H. Abdoul-Carime, J. Langer, M. A. Huels, and E. Illenberger, Eur. Phys. J. D 35, 399–404 (2005).
- ³⁰P. D. Burrow, G. A. Gallup, A. M. Scheer, S. Denifl, S. Ptasinska, T. Mark, and P. Scheier, J. Chem. Phys. **125**(12), 124310 (2006).
- ³¹D. Huber, M. Beikircher, S. Denifl, F. Zappa, S. Matejcik, A. Bacher, V. Grill, T. D. Märk, and P. Scheier, J. Chem. Phys. 125, 084304 (2006).
- ³²J. Kopyra, H. Abdoul-Carime, F. Kossoski, and M. T. d. N. Varella, Phys. Chem. Chem. Phys. **16**(45), 25054–25061 (2014).
- ³³J. Kopyra and H. Abdoul-Carime, J. Chem. Phys. 144, 034306 (2016).

- ³⁴ J. Kopyra, K. K. Kopyra, H. Abdoul-Carime, and D. Branowska, J. Chem. Phys. 148(23), 234301 (2018).
- ³⁵J. H. Hendricks, S. A. Lyapustina, H. L. de Clercq, J. T. Snodgrass, and K. H. Bowen, J. Chem. Phys. **104**(19), 7788–7791 (1996).
- ³⁶X. Li, K. H. Bowen, M. Haranczyk, R. A. Bachorz, K. Mazurkiewicz, J. Rak, and M. Gutowski, J. Chem. Phys. **127**(17), 174309 (2007).
- ³⁷ J. Schiedt, R. Weinkauf, D. M. Neumark, and E. W. Schlag, Chem. Phys. 239, 511–524 (1998).
- ³⁸ J. Simons, J. Phys. Chem. A **112**(29), 6401–6511 (2008).
- ³⁹O. H. Crawford, Mol. Phys. **20**(4), 585–591 (1971).
- ⁴⁰R. A. Bachorz, W. Klopper, M. Gutowski, X. Li, and K. H. Bowen, J. Chem. Phys. 129(5), 054309 (2008).
- ⁴¹ A. Kunin and D. M. Neumark, Phys. Chem. Chem. Phys. **21**(14), 7239–7255 (2019).
- ⁴²X. Li, J. Chen, and K. H. Bowen, J. Chem. Phys. **134**(7), 074304 (2011).
- ⁴³O. Dolgounitcheva, V. Zakrzewski, and J. Ortiz, J. Chem. Phys. **134**(7), 074305 (2011).
- ⁴⁴ E. Matthews, R. Cercola, G. Mensa-Bonsu, D. M. Neumark, and C. E. Dessent, J. Chem. Phys. **148**(8), 084304 (2018).
- ⁴⁵S. B. King, M. A. Yandell, A. B. Stephansen, and D. M. Neumark, J. Chem. Phys. **141**(22), 224310 (2014).
- ⁴⁶ W.-L. Li, A. Kunin, E. Matthews, N. Yoshikawa, C. E. Dessent, and D. M. Neumark, J. Chem. Phys. **145**(4), 044319 (2016).
- ⁴⁷ M. A. Yandell, S. B. King, and D. M. Neumark, J. Am. Chem. Soc. **135**(6), 2128–2131 (2013).
- ⁴⁸ S. B. King, M. A. Yandell, and D. M. Neumark, Faraday Discuss. **163**, 59–72 (2013).
- ⁴⁹ A. B. Stephansen, S. B. King, Y. Yokoi, Y. Minoshima, W.-L. Li, A. Kunin, T. Takayanagi, and D. M. Neumark, J. Chem. Phys. **143**(10), 104308 (2015).
- ⁵⁰ A. Kunin, V. S. McGraw, K. G. Lunny, and D. M. Neumark, J. Chem. Phys. 151(15), 154304 (2019).
- ⁵¹ A. L. Kunin, W. L. Li, and D. M. Neumark, J. Chem. Phys. **149**(8), 084301 (2018).
- (2018). ⁵²M. Koga, M. Asplund, and D. M. Neumark, J. Chem. Phys. **156**, 024302 (2022).
- ⁵³R. Cercola, E. Matthews, and C. E. Dessent, Mol. Phys. **117**(21), 3001–3010 (2019)
- ⁵⁴ K. O. Uleanya, R. Cercola, M. Nikolova, E. Matthews, N. G. K. Wong, and C. E. Dessent, Molecules **25**(14), 3157 (2020).
- ⁵⁵K. O. Uleanya and C. E. Dessent, Phys. Chem. Chem. Phys. **23**(2), 1021–1030 (2021)
- ⁵⁶ A. V. Davis, R. Wester, A. E. Bragg, and D. M. Neumark, J. Chem. Phys. 118(3), 999–1002 (2003).
- ⁵⁷ A. E. Bragg, J. R. R. Verlet, A. Kammrath, O. Cheshnovsky, and D. M. Neumark, J. Am. Chem. Soc. **127**(43), 15283–15295 (2005).
- ⁵⁸W. Wiley and I. H. McLaren, Rev. Sci. Instrum. 26(12), 1150–1157 (1955).
- ⁵⁹ V. Dribinski, A. Ossadtchi, V. A. Mandelshtam, and H. Reisler, Rev. Sci. Instrum. **73**(7), 2634–2642 (2002).
- ⁶⁰ M. J. Frisch, G. W. Trucks, H. B. Schlegel, G. E. Scuseria, M. A. Robb, J. R. Cheeseman, G. Scalmani, V. Barone, G. A. Petersson, H. Nakatsuji, X. Li, M. Caricato, A. V. Marenich, J. Bloino, B. G. Janesko, R. Gomperts, B. Mennucci, H. P. Hratchian, J. V. Ortiz, A. F. Izmaylov, J. L. Sonnenberg, D. Williams-Young, F. Ding, F. Lipparini, F. Egidi, J. Goings, B. Peng, A. Petrone, T. Henderson, D. Ranasinghe, V. G. Zakrzewski, J. Gao, N. Rega, G. Zheng, W. Liang, M. Hada, M. Ehara, K. Toyota, R. Fukuda, J. Hasegawa, M. Ishida, T. Nakajima, Y. Honda, O. Kitao, H. Nakai, T. Vreven, K. Throssell, J. A. Montgomery, Jr., J. E. Peralta, F. A. Keith, R. Kobayashi, J. Normand, K. Raghavachari, A. P. Rendell, J. C. Burant, S. S. Iyengar, J. Tomasi, M. Cossi, J. M. Millam, M. Klene, C. Adamo, R. Cammi, J. W. Ochterski, R. L. Martin, K. Morokuma, O. Farkas, J. B. Foresman, and D. J. Fox, Gaussian 16, Rev. A.03, Gaussian, Inc., Wallingford, CT, 2016.
- ⁶¹ K. A. Peterson, B. C. Shepler, D. Figgen, and H. Stoll, J. Phys. Chem. A 110(51), 13877–13883 (2006).

- 62 S. B. King, A. B. Stephansen, Y. Yokoi, M. A. Yandell, A. Kunin, T. Takayanagi,
- and D. M. Neumark, J. Chem. Phys. **143**(2), 024312 (2015). ⁶³R. J. Peláez, C. Blondel, C. Delsart, and C. Drag, J. Phys. B: At., Mol. Opt. Phys. 42, 125001 (2009).
- ⁶⁴T. Sommerfeld, J. Phys. Chem. A **108**(42), 9150–9154 (2004).
- ⁶⁵S. J. Jishnu Narayanan, D. Tripathi, and A. K. Dutta, J. Phys. Chem. Lett. **12**(42), 10380-10387 (2021).
- ⁶⁶T. Baer, W. L. Hase, and L. William, Unimolecular Reaction Dynamics: Theory and Experiments (Oxford University Press on Demand, 1996).
- ⁶⁷R. G. Gilbert and S. C. Smith, Theory of Unimolecular and Recomination Reactions (Publishers' Business Services, 1990).
- ⁶⁸ T. Beyer and D. F. Swinehart, Commun. ACM **16**(6), 379 (1973).
- ⁶⁹S. E. Stein and B. Rabinovitch, J. Chem. Phys. **58**(6), 2438–2445
- (1973). ⁷⁰ A. Kunin, W.-L. Li, and D. M. Neumark, Phys. Chem. Chem. Phys. **18**, 33226
- (2016).
 ⁷¹R. A. Bachorz, W. Klopper, and M. Gutowski, J. Chem. Phys. **126**(8), 085101